J Solid State Electrochem (2010) 14:1621–1627
DOI 10.1007/s10008-010-1006-z

ORIGINAL PAPER

Electrochemical behavior of silver-impregnated Al-pillared smectite in alkaline solution

Zorica Mojović · Aleksandra Milutinović-Nikolić · Predrag Banković · Slavko Mentus · Dušan Jovanović

Received: 12 November 2009 / Revised: 17 December 2009 / Accepted: 7 January 2010 / Published online: 29 January 2010

Abstract In order to enhance silver effectiveness for oxygen reduction reaction, pillared clay was used as a support for silver nanodispersion. Silver particles incorporation into pillared clay pores was attempted by impregnation/thermal degradation technique. X-ray diffraction as well as adsorption-desorption isotherms confirmed that pillaring procedure was successful. Scanning electron microscopy evidenced that a part of silver appeared outside the pillared clay cavities. Ag-pillared clay composite homogenized with 10 wt.% of nanodispersed carbon black (Vulcan), was applied on a flat glassy carbon surface and used as an electrode material. Oxygen reduction reaction was investigated in an O_2-saturated aqueous 0.1 M NaOH solution.

Keywords Clays · Electrochemistry · Silver · Oxygen reduction

Introduction

Electrocatalytic effectiveness of silver for oxygen reduction in alkaline solutions is comparable to one displayed by platinum [1]. This reaction has been investigated on different silver-based catalysts. McIntyre and Peck investigated the oxygen reduction kinetics on the single-crystal metal electrodes [2]. Damjanović et al. found that pretreatment of the silver electrode significantly affects the kinetics of the reduction [3]. Silver alloys [4, 5] as well as silver nanodispersion over carbon [6, 7] have also been investigated. Silver catalytic effectiveness has also been enhanced by supporting on TiO_2 [8].

Increasing the surface area of the catalyst by reducing particle size represents a recognized means for the catalytic activity improvement. Aluminosilicates, such as zeolites and clays, containing cavities with nanometric dimensions, represent a specific support for metal clusters incorporation, limiting the cluster growth to the dimensions of the cavities. Clays are particularly interesting for the metal incorporation due to their wide range of pore diameters. One of the clay properties is swelling. In order to use clay for metal incorporation, fixed porosity is required. Pillaring process, based on the intercalation properties of the clay matrix, involves exchange of interlayer cations with polyhydroxy metallic precursor [9]. Upon calcinations. these precursors are converted to metal oxide pillars between the clay layers keeping them apart at a definite distance.

In this paper, Al-pillared smectite clay was synthesized. The methods available to incorporate metal clusters into the clay cavities are either ion exchange followed by reduction [10–12], or impregnation by thermodegradable salt solution [13, 14] followed by drying and thermal degradation. The technique of Al-pillared clay impregnation by Ag-acetylacetonate dissolved in acetone was used to incorporate silver within the cavities. Ag-modified pillared clay, with addition of carbon black (Vulcan) that provides satisfying electronic conductivity, was investigated as catalyst for oxygen reduction reaction in alkaline solution.

Z. Mojović (✉) · A. Milutinović-Nikolić · P. Banković · D. Jovanović
IChTM-Department of Catalysis and Chemical Engineering, Belgrade University,
Njegoševa 12,
Belgrade, Serbia
e-mail: zoricam@nanosys.ihtm.bg.ac.rs

S. Mentus
Faculty of Physical Chemistry, Belgrade University,
Studentski Trg 12,
Belgrade, Serbia

Experimental

Pillaring procedure

Starting material was Wyoming-type Na-montmorillonite (Clay Minerals Society Source Clay denoted as SWy-2).

The process of pillaring was carried out according to a common procedure [15]. Pillaring solution was prepared by adding adequate volumes of 0.2 M NaOH to 0.2 M Al $(NO_3)_3$ in order to achieve molar ratio OH^-/Al^{3+}=2.0. The procedure included continuous stirring at 60 °C for 3 h and at room temperature overnight. In the next step, the pillaring solution was slowly added into 1 wt.% clay dispersion in distilled water. The amount of added pillaring solution was calculated to reach Al^{3+}/clay ratio of 20 mmol g^{-1}. After being rigorously stirred at 80 °C for 3 h, the final suspension was stirred at room temperature overnight. The suspension was filtered through a Büchner funnel while hot. The obtained cake was rinsed with hot distilled water until the filtrate was NO_3^- free (tested by UV-Vis spectrophotometry), and finally, air-dried overnight at 110 °C. It was then calcined at 350 °C for 2 h. The obtained material was referred as Al-SWy-2.

Impregnation procedure

Procedure given for thermal decomposition of noble metal acetylacetonates used for the deposition of noble metal clusters onto the surface of a solid support [16], was adapted by here involved authors aiming to introduce noble metal clusters into zeolite cavities [17, 18], and presently into pillared clay pores. Shortly, after heating up to 350 °C in order to remove adsorbed water and subsequent cooling to room temperature in a dry atmosphere, the clay sample was slightly wetted with diluted solution of silver acetylacetonate in acetone. The sample was then dried at 90 °C to evaporate acetone and heated at 350 °C with aim of both decomposition of Ag-acetylacetonate and removal of its gaseous decomposition products. This temperature is within the temperature interval that corresponds to thermal stability of the clay. The impregnation/decomposition procedure was repeated about ten times until the Ag/pillared clay weight ratio of 0.1 was achieved. The obtained material was referred as Al-SWy-2-Ag.

Characterization

The X-ray diffraction (XRD) patterns for powders of SWy-2, Al-SWy-2, and Al-SWy-2-Ag were obtained using a Philips PW 1710 X-ray powder diffractometer with a Cu anode (λ=0.154178 nm).

Nitrogen adsorption-desorption isotherms were determined on a Sorptomatic 1990 Thermo Finningen at −196 °C. The samples were outgassed at 160 °C, during 20 h. WinADP software was used to analyze obtained isotherms.

SEM experiments were performed on a JSM-6460LV electron microscope (JEOL, Japan) operating at an accelerating voltage of 25 kV and the samples were coated with Au thin film.

Electrocatalytic test

In order to use the Al-SWy-2Ag as electrode material, the sample was homogeneously dispersed in 5 wt.% Nafion solution in a mixture of isopropyl alcohol and water using ultrasonic bath. The electronic conductivity of the samples was enhanced by adding 10 wt.% of carbon black Vulcan XC72 (Cabot Corp.) into the initial suspension. Droplets of these suspensions were placed on the surface of a glassy carbon rotating disc electrode. After the solvent removal by evaporation at 90 °C, the sample particles were uniformly distributed on the glassy carbon support in a form of thin layer.

Electrochemical performance of this material was investigated in a 0.1 M NaOH solution using rotating disc technique in a three-electrode glass cell with Ag/AgCl in 1 M KCl as a reference electrode while a platinum foil served as a counter electrode. Device used for the electrochemical measurements was a 757 VA Computrace Metrohm.

Results and discussion

X-ray diffraction

According to X-ray diffraction patterns (Fig. 1), the following phases were identified in the investigated

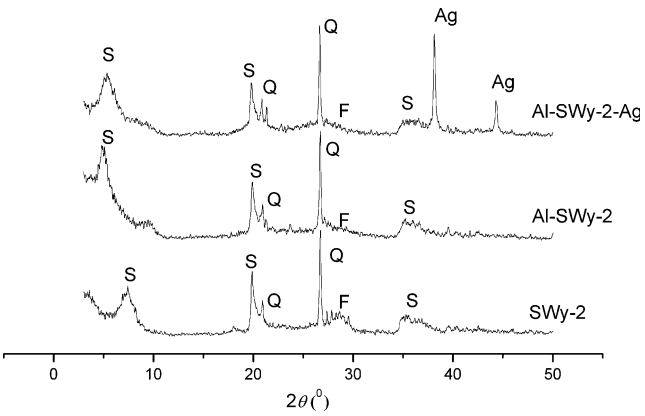

Fig. 1 X-Ray diffractograms of the starting smectite (*SWy-2*), pillared smectite (*Al-SWy-2*) and silver-impregnated pillared smectite (*Al-SWy-2-Ag*). *S* smectite, *Q* quartz, *F* feldspar, *C* calcite

samples: smectite, quartz, feldspar and a small amount of amorphous phase [19].

The (001) smectite peak appeared in the region of $2\theta < 10°$. For SWy-2 sample this peak appeared at 6.9° (2θ) corresponding to the basal spacing of 1.28 nm. The pillaring process increased and fixed basal spacing between clay sheets causing shifting of the *d(001)* peak toward lower 2θ values. Therefore, the *d(001)* diffraction line for the pillared sample Al-SWy-2 at 5.4°(2θ), corresponding to basal spacing of 1.64 nm, confirms that the pillaring process was successful.

The peak sharpness indicates that the intercalation process was homogeneous and resistant to the calcination treatment [20]. Difractogram of the silver-impregnated pillared clay shows somewhat broader *d(001)* diffraction line. According to JCPDS (Joint Committee on Powder Diffraction Standards)[19] diffraction lines of crystalline silver correspond to peaks at 38.1 and 44.3° (2θ). The entire width at half maximum of these peaks is relatively small indicating that silver is present in a form of particles with size up to couple of hundreds of nanometer. The crystalline structure of the pillared clay was preserved after the impregnation procedure, but somewhat lower signal/noise ratio could indicate amorphization at local level.

Adsorption-desorption isotherms

Nitrogen adsorption-desorption isotherms obtained for the investigated samples are presented in Fig. 2. The isotherm of the starting clay (SWy-2) is reversible at low relative pressures, while at higher relative pressures ($p/p_0 \geq 0.4$) it shows H3 type hysteresis [21]. According to IUPAC classification it corresponds to the type 2 isotherms which are obtained for either slit-shaped pores or, as in this case, assemblages of many particles. This type of isotherm indicates unrestricted monolayer-multilayer nitrogen adsorption to occur at high p/p_0.

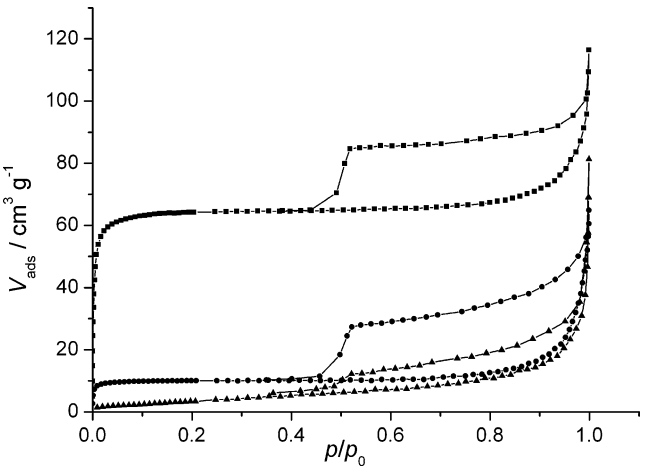

Fig. 2 N_2 adsorption-desorption isotherms for SWy-2 (*circles*), Al-SWy-2 (*squares*) and Al-SWy-2-Ag (*triangles*)

Pillaring process introduces permanent porosity into clay material, with new pores usually developed in the microporous region. Therefore, one might expect pillared clay to exhibits type 1 adsorption isotherm. Isotherm obtained for Al-SWy-2 rises sharply at low relative pressures and reaches plateau. However, it is not reversible exhibiting H3 type hysteresis at higher p/p_0. It actually might be considered as a combination of type 1 and type 2 isotherms. Adsorption isotherm of pillared clay impregnated with silver (Al-SWy-2-Ag) is type 2, indicating loss in microporosity.

Textural properties calculated from the adsorption isothem data are presented in Table 1.

The specific surface area of the samples, S_{BET}, was calculated according to Brunauer, Emmett, Teller method [22] while the total pore volume ($V_{0.98}$) was calculated according Gurvich method [21]. Dubinin-Radushkevich [23] (DR) method was applied to adsorption isotherms in order to obtain micropore volume ($V_\mu{}^D$). The pore distribution in the micropore range was determined according Horwath–Kawazoe (HK) model for slit-shaped pores [24], while Barret, Joyner and Halenda (BJH) model was used for pores in the mesopore range.

A large increase in the specific surface area is observed between the starting and the pillared sample. After the impregnation with silver, newly developed surface area was reduced even below the value of the starting sample. Micropore volume increased from 0.016 cm^3 g^{-1}, for the starting sample, to 0.102 cm^3 g^{-1} for the pillared sample. Theoretically, maximum micopore volume that could be obtained for the aluminium pillared smectites is about 0.12 cm^3 g^{-1} [25]. Micropore volume of Al-SWy-2-Ag is negligible. The HK micropore diameter of the pillared sample is 0.76 nm, while the starting clay and silver impregnated sample have pores with diameters around 2 nm. Mesopore diameter, as well as mesopore volume, is not significantly affected neither by pillaring procedure nor by impregnation. Cumulative volume changes reflect changes in micropore volume.

The increase in the surface areas and micropore volume was expected for the pillared sample, since the pillaring procedure promotes microporosity. Influence of impregnation of Al-pillared clays with metal on their textural properties was investigated by Barrera-Vargas et al. [26] Al-pillared clays were impregnated with platinum up to 1.8 wt.%. Increase of platinum content in pillared clay lead to continuous decrease of textural properties. In this work, pillared clay was impregnated with substantially higher metal content (10 wt.%). The obtained results are in good agreement with observation presented by Barrera-Vargasa et al. It might be concluded that the impregnation procedure

Table 1 The textural properties of samples based on the analysis of nitrogen adsorption isotherms

Sample	SWy-2	Al-SWy-2	Al-SWy-2-Ag
S_{BET} (m^2g^{-1})	33	198	14
V_{μ}^{D} (cm^3g^{-1})	0.016	0.102	0.004
$V_{0.98}$ (cm^3g^{-1})	0.099	0.178	0.122
HK diameter (nm)	2.06	0.76	1.94
BJH diameter (nm)	3.92	3.93	3.95
V_{meso}(cm^3g^{-1})	0.09	0.08	0.06

S_{BET} specific surface area, V_{μ}^{D} micropore volume, $V_{0.98}$ total pore volume, *HK diameter* micropore diameter determined according Horwath–Kawazoe model; *BJH diameter* mesopore diameter obtained according Barret, Joyner and Halenda model; V_{meso} mesopore volume

lead to complete occupation of micropore by silver atoms disabling entrance of nitrogen molecules. However, the pillared clay was impregnated with 10 wt.% of silver. It means that for each gram of clay 0.1 g of silver was added. Taking into account silver density, which is 10.45 gcm^{-3}, it can be calculated that this amount of silver has volume of about 0.01 cm^{-3}. Available volume in pillared clay is ten times greater. Therefore, total micropore volume decrease cannot be ascribed to filling with silver. Having in mind XRD analysis, it can be concluded that the impregnation procedure with acetyacetonate influenced smectite crystal structure at local level leading to partial amorphization.

Scanning electron micrography

The SEM microphotographs of the investigated samples are presented in Fig. 3.

Layered structure of the starting sample is clearly observable in Fig. 3. According to microphotographs it seems that the pillaring process caused some structural changes of starting clay leading to formation of particles. In Fig. 3c is presented pillared clay impregnated with silver. At least part of silver in pillared clay impregnated with silver is present at outer clay surface in the form of particles with diameter of 200–500 nm. This finding is in accordance with XRD analysis where sharp diffraction peaks indicated presence of rather large silver clusters. The presence of silver clusters undoubtedly indicates that the loss of microporosity is not a consequence of complete silver incorporation into the micropores. The loss of microporosity is most probably caused by partial structure degradation.

The impregnation of pillared clay with silver was done in order to obtain silver nanowires between clay layers. According to the XRD and SEM results, this aim was not completely fulfilled. Nevertheless, the partial silver incorporation into the pillared clay could occur. Therefore, the obtained material has been subjected to the further electrochemical investigation.

Electrochemical behavior

The steady-state cyclovoltammogram with composite electrode layer (mixture of Al-SWy-2-Ag with carbon black in Nafion solution), obtained after 20–30 polarization cycles, in nitrogen purged 0.1 M NaOH, within the voltage window shorter than that of water splitting, is presented in Fig. 4. The first anodic peak at +0.44 V vs. Ag/AgCl is related to the formation of Ag_2O (standard potential, E^o= 0.342 V vs. SHE), and its reverse cathodic peak lies at −0.1 V. The existence of shoulder on this cathodic peak is a consequence of complex structure of the anodic peak. The anodic peaks related to the formation of AgO, (E^o=0.599 V vs. SHE) and Ag_2O_3 (E^o=0.74 V vs. SHE) are not clearly distinguished from those corresponding to oxygen evolution reaction at 1.0 V. Cathodic peaks at +0.45 V and +0.23 V (vs. Ag/AgCl) corresponding to reduction of these higher valence silver oxides. In the cathodic polarization direction, at the potential of −0.4 V, reduction of oxygen, which remained in the clay pores, is observable. The height of this peak may be significantly reduced by switching off electrode rotation.

The diagram in Fig. 4 is similar to that for bulk polycrystalline silver electrode in alkaline solution [27, 28], in this work, however, during anodic polarization, the potential did not exceed 0.8 V vs Hg/HgO, 0.1 M NaOH,

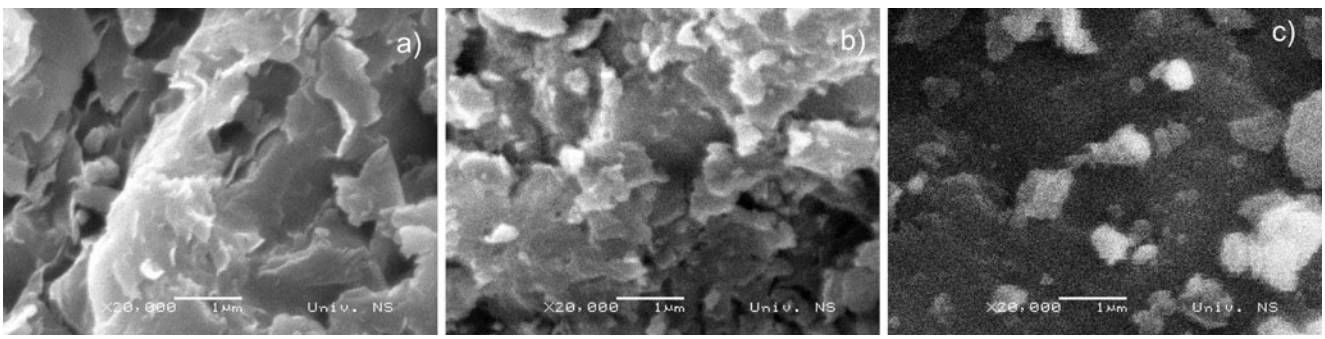

Fig. 3 The SEM microphotographs of SWy-2 (**a**), Al-SWy-2 (**b**) and Al-SWy-2-Ag (**c**)

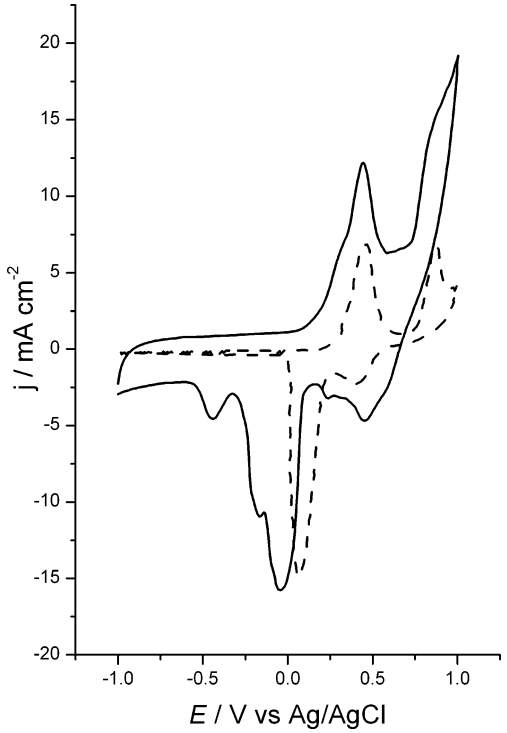

Fig. 4 Steady-state voltammogram of Al-Swy-2-Ag composite electrode material in deaerated 0.1 M NaOH solution, recorded at a polarization rate of 50 mV s^{-1} (*solid line*). Voltammogram of polycrystalline silver electrode in deaerated 0.1 M NaOH solution, recorded at a polarization rate of 20 mV s^{-1} (*dashed line*) is presented for comparison

(≈0.7 V vs Ag/AgCl) and thus the peaks corresponding to Ag_2O_3 were not registered.

The stability of composite electrode layer applied on carbon glass rotating disc electrode was evaluated by cycling in 0.1 M NaOH in potential range between −1 V and +1 V vs. Ag/AgCl at 50 mV/s and rotation rate 800 rpm. As earlier mentioned, the steady-state cyclovoltammogram was obtained after 20–30 polarization cycles. After that the CV s showed stable behavior even up to 100 cycles of continuous use.

Oxygen reduction reaction Electrocatalytic activity of Al-Swy-2-Ag toward oxygen reduction was investigated in oxygen-saturated 0.1 M NaOH. Current-potential (*j-E*) curves recorded using cathodic sweep, at various rotation rates, are presented in Fig. 5. For comparison purposes, the voltammogram of monocrystalline Ag(100) in the same solution [29] recorded at rotation rate of 1,600 rpm is presented too.

The *j-E* dependence for Ag(100), being known to display the highest activity toward ORR, does not overlap with here recorded curve obtained for the same rotation rate. Nevertheless, the investigated composite electrode material has shown rather good activity toward ORR. The shape of the voltammograms indicates that the process was controlled by diffusion.

It is already known that, in alkaline solutions, oxygen reduction reaction on bulk silver surface follows the $4e^-$ path. For dispersed silver electrode, Yang et al. and Zhou et al. [6, 30] suggested that oxygen reduction on silver particles may follow $4e^-$ route at crystal face sites and $2e^-$ one at the edge and the corner sites, while the size of the Ag particles affects catalytic activity for the $4e^-$ and $2e^-$reduction of oxygen. In view of these results, on very developed silver surface like the one formed in here studied composite material, one might expect a great number of corner and edge sites with their role in defining the electrode reaction path.

In order to prove both the type of reaction control, and the number of electrons taking part in ORR on the composite electrode under investigation, the Levich plot was considered, according to the equation:

$$j_l = 0.62nFD^{2/3}v^{-1/6}\omega^{1/2}C \quad (1)$$

or, in shorter form :

$$j_l = B\omega^{1/2} \quad (1')$$

where ν represents the kinematic viscosity, i.e. viscosity divided by density, and ω is angular rotation frequency ($\omega = 2\pi f$, where f is rotation frequency), while C and D are

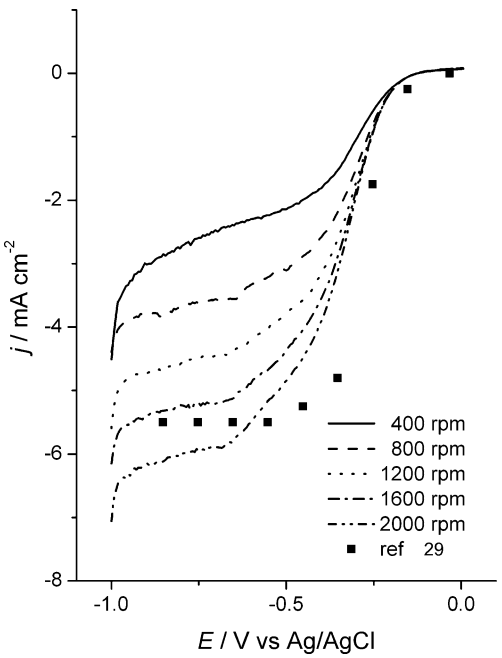

Fig. 5 *j-E* curves for ORR on composite electrode Al-SWy-2-Ag in oxygen-saturated 0.1 M NaOH, at a polarization rate of 5 mV s^{-1} and different rotation rates assigned in the legend. The *squares* present the data for Ag(100) crystallographic plane at rotation rate of 1,600 rpm, taken from ref. [29]

concentration and diffusion coefficient of dissolved oxygen. This relation is valid for the processes controlled exclusively by mass transfer (diffusion). The reaction path of ORR, which may be expected to vary between $2e^-$ and $4e^-$ one, may be checked on the basis of the slope B of Levich plot (1'), which, for other values being constant, depends only on the number of electrons n.

The kinematic viscosity of 0.1 M NaOH solution used here is very close to that of water and thus may be taken to amount to 0.01 $cm^2 s^{-1}$. For usual values of solubility of O_2 in water of 1.18×10^{-3} mol dm^{-3}, and diffusion coefficient of O_2 of $1.95\times10^{-5} cm^2 s^{-1}$, the calculated slope B amounts to 0.436 mA $cm^{-2} rad^{-1/2} s^{1/2}$ for n=4 and 0.219 mA cm^{-2} $rad^{-1/2} s^{1/2}$ for n=2.

Figure 6 shows that the experimental data in the region of current plateau (−0.7 V) obey very well the Eq. 1. This fact confirms that the process was controlled by diffusion. For the voltage belonging to the region of diffusion control, the slope of the line in Fig. 6 amounts to 0.426 mA $cm^{-2} s^{1/2}$, which evidences that oxygen reduction path is close to the $4e^-$ one, i.e., the influence of corner and edge sites, if present at all, is not dominant.

A comparison of the electrocatalytic activity of the composite electrode for the ORR can be made by comparing the obtained Tafel slope with literature data for other silver-based materials. The Tafel slope obtained for Al-Swy-2-Ag electrode amounts 52 mV dec^{-1} and 63 mV dec^{-1} for polycrystalline silver electrode. The data obtained in the literature reports Tafel slopes of 84 mV dec^{-1} for Ag/C [31], 98 mV dec^{-1} for monocrystalline Ag (100) [29], 70 mV dec^{-1} for Ag/C [32], 94 mV dec^{-1} for silver nanowires [33].

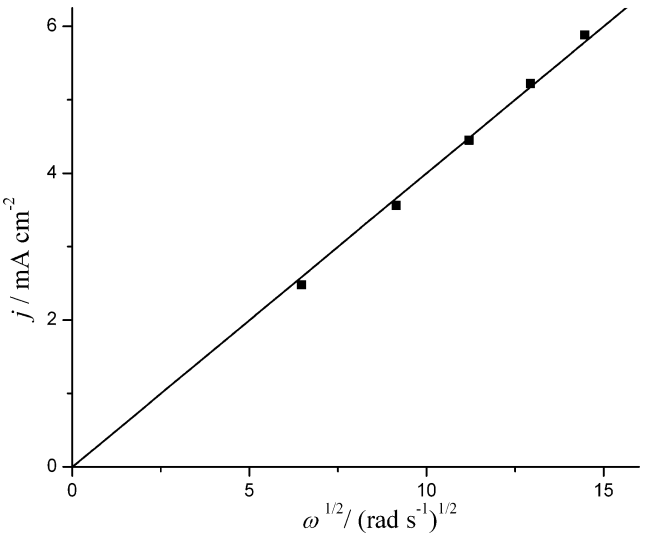

Fig. 6 Current density versus square root of angular frequency for ORR in oxygen-saturated 0.1 M NaOH solution, at the potential of −0.7 V vs. Ag/AgCl, Cl^-

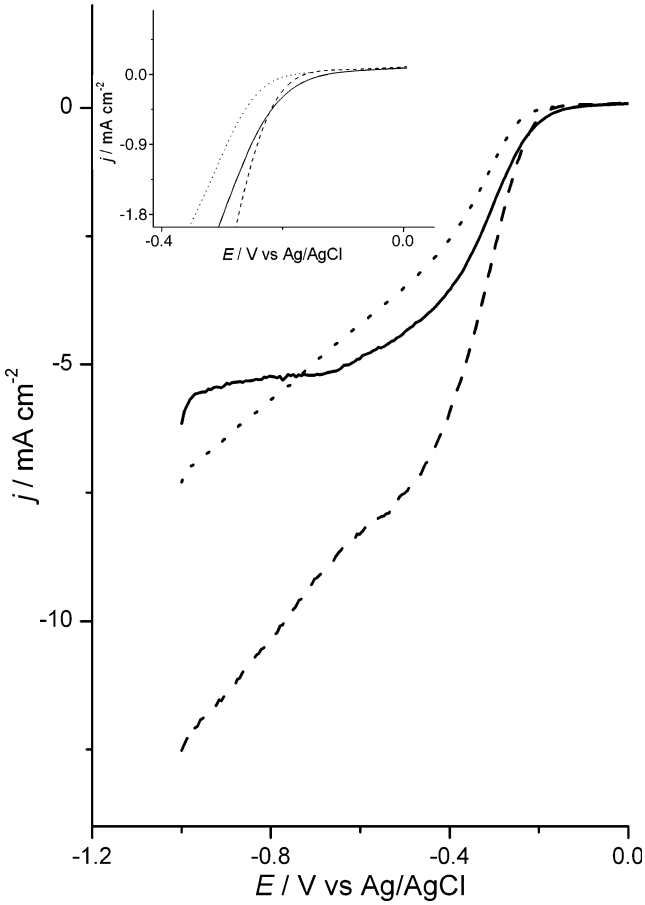

Fig. 7 *j-E* curves for ORR on composite electrode Al-SWy-2-Ag (*solid curve*), Al-Swy-2 (*dotted curve*) and carbon black-nafion-modified carbon glass electrode (*dashed curve*) in oxygen-saturated 0.1 M NaOH, at a polarization rate of 5 mV s^{-1}, and rotation rate of 1,600 rpm. The *inserted picture* represents the onset potential region

Another comparison can be obtained by comparing onset potential for ORR. In comparing the electrocatalytic performance, electrodes with more positive ORR onset potential will perform better as cathode catalysts. The onset potential of Al-Swy-2-Ag electrode is −0.11 V vs. Ag/AgCl. The literature data reports the onset potential of −0.05 for monocrystalline Ag (100) [29], −0.11 V for Ag/C [34], −0.027 V for Ag/CNT [35], −0.17 V for silver nanowires [33].

Therefore, it must be concluded that he electrocatalytic activity of the investigated composite material is somewhat lower in comparison with other silver-based materials reported in the literature.

Blank experiments In order to distinguish contribution of different components of investigated composite Nafion-carbon black-Al-SWy-2-Ag electrode two blank experiments have been performed. The first one investigated the electroactivity for ORR of pillared clay Al-Swy-2 (without silver impregnation) prepared in the same manner as Al-Swy-2-Ag. The second one investigated the electroactivity

for ORR of carbon black-nafion modified carbon glass electrode. The obtained current-potential (*j-E*) curves recorded using cathodic sweep at 5 mV s^{-1} and 1,600 rpm are presented at Fig. 7 together with *j-E* curve obtained for Al-Swy-2-Ag at the same conditions. As expected, the lowest current was obtained for Al-Swy-2 electrode, and the highest for the carbon black-modified electrode. However, no plateau indicating diffusion limitation was reached for Al-SWy-2 and carbon black-modified electrode. Furthermore, Al-Swy-2-Ag has showed the most positive onset potential for ORR. The Tafel slopes amounted 39 mV dec^{-1}, 43 mV dec^{-1} and 52 mV dec^{-1} for the Al-Swy-2, carbon black-modified electrode and Al-Swy-2-Ag electrode, respectively. It can be concluded that enhanced electroactivity of the composite Nafion-carbon black-Al-SWy-2-Ag electrode is consequence of combined effects of increased area of the electrode and the presence of the silver particles.

Conclusions

Composite electrode material based on Al-pillared smectite and silver dispersed both within and out of smectite pores, in N_2 purged 0.1 M NaOH solution yielded cyclic voltammogram that corresponds to pure silver of well developed real surface area. The same electrode material in oxygen-saturated 0.1 M NaOH solution, using rotating disc technique, yielded voltammograms that indicate four-electron route of oxygen reduction reaction. The impregnation/thermal degradation technique applied for silver deposition on pillared clay did not lead to expected silver nanowire formation trough pillared clay layer. The electrocatalytic activity of the obtained material is somewhat lower in comparison with other silver-based materials reported in the literature.

Acknowledgment This work was supported by the Ministry of Science of Republic Serbia, contracts No. 166001B, No. 142019 and 142047.

References

1. Hacker V, Wallnöfer E, Baumgartner W, Schaffer T, Besenhard JO, Schröttner H, Schmied M (2005) Electrochem Commun 7:377
2. McIntyre J, Peck W (1984) Electrochemistry at single-crystal metal electrodes. Electrocatalytic effects on surface atomic structure, defects and adatoms on oxygen reduction. In: McIntyre J, Weaver M, Yeager E (eds) The chemistry and physics of electrocatalysis. The Electrochemical Society, Pennington, pp 102–130
3. Šepa D, Vojnović M, Damjanović A (1970) Electrochim Acta 15:1355
4. Arul Raj I, Vasu K (1993) J Appl Electrochem 23:728
5. Lee H, Shim J-P, Shim M-J, Kim S-W, Lee J-S (1996) Mater Chem Phys 45:238
6. Yang YF, Zhon YH (1995) J Electroanal Chem 397:271
7. Cassagneau T, Fendler J (1999) J Phys Chem B 103:1789
8. Bosković I, Mentus S, Pješčić M (2006) Electrochim Acta 51:2793
9. Kloprogge J (1998) J Porous Mater 5:5
10. Maes A, Cremers A (1977) J Chem Soc Perkin Trans 1 73:1807
11. Ferris A, Jepson W (1975) J Colloid Interface Sci 51:245
12. Coleman N, Bishop A, Booth S, Nicholson J (2009) J Eur Ceram Soc 29:1109
13. Ramaswamy V, Malwadkar S, Chilukuri S (2008) Appl Catal B 84:21
14. Belver C, Mata G, Trujillano R, Vicente M (2008) Catal Lett 123:32
15. Catrinescu C, Teodosiu C, Macoveanu M, Miehe-Brendlé J, Le Dred R (2003) Water Res 37:1154
16. Okumura M, Tanaka K, Ueda A, Haruta M (1997) Solid State Ionics 95:143
17. Mentus S, Mojović Z, Cvjetićanin N, Tešić Z (2003) Fuell Cells 3:15
18. Mojovic Z, Mentus S, Cvjeticanin N, Tesic Z (2004) Mat Sci Forum 453–454:257
19. International Center for Diffraction Data – Joint Committee on Powder Diffraction Standards Powder diffraction data (1990) Swarthmore. PA, USA
20. Sánches A, Montes M (1998) Microporous Mesoporous Mater 21:117
21. Rouquerol F, Rouquerol J, Sing K (1999) Adsorption by Powders and Porous Solids. Academic Press, London
22. Gregg S, Sing K (1967) Adsorption. Academic Press, New York, Surface Area and Porosity
23. Dubinin M (1975) Progress in surface and membrane science. Academic Press, New York
24. Horwath G, Kawazoe K (1983) J Chem Eng Jpn 16:470
25. Brotas de Carvalho M, Pires J, Carvalho A (1996) Microporous Mater 6:65
26. Barrera-Vargas M, Valencia-Rios J, Vicente M, Korili S, Gil A (2005) J Phys Chem B 109:23461
27. Nagle L, Ahern A, Burke L (2002) J Solid State Electrochem 6:320
28. Popkirov G, Burmeister M, Schindler R (1995) J Electroanal Chem 380:249
29. Blizanac B, Ross P, Markovic N (2006) J Phys Chem B 110:4735
30. Yang YF, Zhou YH (1996) J Electroanal Chem 415:143
31. Chatenet M, Genies-Bultel L, Aurousseau M, Durand R, Andolfatto F (2002) J Appl Electrochem 32:1131
32. Lima FHB, de Castro JFR, Ticianelli EA (2006) J Power Sources 161:806
33. Ni K, Chen l, Lu G (2008) Electrochem Commun 10:1027
34. Demarconnay L, Coutanceau C, Léger JM (2004) Electrochim Acta 49:4513
35. Kostowskyj MA, Gilliam RJ, Kirk DW, Thorpe SJ (2008) J Hydrogen Ene 33:5773